

DOI:10.1002/ejic.201403021

Iron(II) Spin-Crossover Complexes with Schiff Base Like Ligands and *N*-Alkylimidazoles

Stephan Schlamp,^[a] Charles Lochenie,^[a] Tobias Bauer,^[a]
Rhett Kempe,^[a] and Birgit Weber*^[a]

Keywords: Iron / Spin crossover / Schiff base ligands / N ligands

Three new iron(II) spin-crossover complexes with N₂O₂-coordinating Schiff base like equatorial ligands and alkylimidazole ligands in the axial positions were synthesised. The chain length of the alkylimidazole was varied from the previously published 1 to 5, 7 and 10 carbon atoms to investigate the influence of the alkyl chain length on the spin-transition

behaviour in solution and in the solid state. The crystal structures of [1(HeptIm)₂] and [1(DecIm)₂] (1 = Fe complex with equatorial Schiff base like ligand; HeptIm = *N*-heptylimidazole, DecIm = *N*-decylimidazole) and the packing of the molecules in the crystals are discussed.

Introduction

Switchable molecules are important for possible applications in the thematic field of sensors, for example. Spin-crossover (SCO) compounds are a class of molecules that are good candidates for this, as they can be switched between the high-spin (HS) and low-spin (LS) states by various means such as changes of temperature or pressure or irradiation with light.^[1] This switching process is accompanied by a change of the properties of the material such as its magnetism or colour. The combination of this ability with additional physical properties such as softness can lead to multifunctional SCO complexes with additional functionalities such as liquid crystallinity, gel formation or nanostructuring through self-assembly.^[2] To achieve this goal, a common method is to add long alkyl chains to the ligands of already established SCO systems.^[3,4] The characterisation of a variety of such SCO compounds showed that the addition of long alkyl chains to the outer periphery often leads to gradual spin transitions. An improved cooperativity with increasing alkyl chain length has only been detected in a few cases.^[5] Additionally, counterions or solvent molecules that can influence SCO behaviour in an unpredictable way are involved in most systems. We also followed this approach by synthesising alkyl-chain-functionalised amphiphilic Schiff base like ligands that were used for the successful synthesis of SCO complexes.^[6] In one case, a cooperative spin transition with hysteresis was observed as result of a highly ordered lipid-layer-like arrangement of the molecules in the crystal packing.^[7]

Here, we present an alternative approach for the synthesis of alkyl-chain-functionalised iron(II) SCO complexes of the ligand system used in our group. For this, *N*-alkylimidazoles were used as axial ligands. The modification of the Schiff base like ligand resulted in amphiphilic complexes, in which the nonpolar alkyl chains point in one direction, and the iron centre is part of the polar head group. For the addition of long alkyl chains to the two axial ligands, rod-like structures of the final complex can be envisioned. Similar structural motifs have already been realised for other SCO systems; however, these systems all feature positively charged complexes with counterions.^[4,8] The advantage of the ligand system presented here is that solely the influence of the alkyl chain length can be investigated.

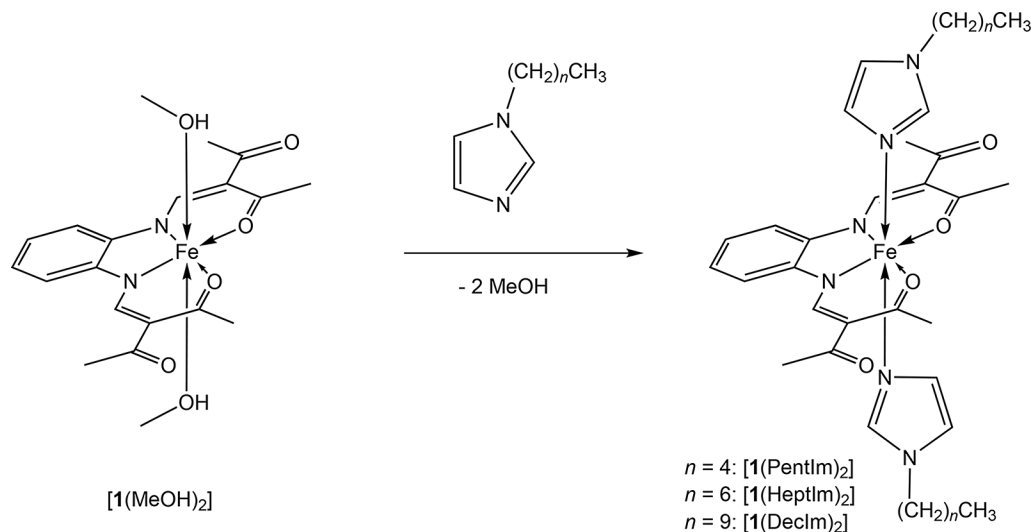
Results and Discussion

Synthesis and General Characterisation

Previously, we demonstrated that iron(II) complexes of the Schiff base like ligands used in our group in combination with *N*-methylimidazole (MeIm) axial ligands show SCO behaviour.^[9,10] The type of spin transition (gradual or abrupt) depends on the method of synthesis. Either the axial ligand, MeIm, was used as the solvent or the starting iron(II) complex was heated to reflux in a mixture of MeIm and methanol. The later strategy was used for two of the alkylimidazole complexes discussed in this manuscript, as the solubility of the iron(II) complex in the pure alkylimidazole is too high, and no solid product could be obtained. The high solubility of the final products made their isolation as pure compounds difficult as washing steps always dissolved the precipitate. Consequently, this step was skipped; the reaction solution was simply decanted, and the

[a] Lehrstuhl für Anorganische Chemie II, Universität Bayreuth, Universitätsstraße 30, NW 1, 95440 Bayreuth, Germany
E-mail: weber@uni-bayreuth.de
<http://www.ac2-weber.uni-bayreuth.de>

Supporting information for this article is available on the WWW under <http://dx.doi.org/10.1002/ejic.201403021>.



Scheme 1. Final step of the synthesis of [1(PentIm)₂], [1(HeptIm)₂] and [1(DecIm)₂].

product was dried in vacuo. As a result, alkyimidazole impurities are often observed in the final products. The final step, the coordination of the corresponding alkyimidazole to the precursor [1(MeOH)₂], is visualised in Scheme 1. The six-step synthesis pathway comprises adapted literature procedures for the synthesis of the alkyimidazoles^[11–13] as well as the previously described syntheses of the Schiff base like ligand^[14] and the methanol precursor complex.^[15]

X-ray Structure Analysis

Single crystals suitable for X-ray structure analysis were obtained for [1(HeptIm)₂] (HeptIm = *N*-heptylimidazole) and [1(DecIm)₂] (DecIm = *N*-decylimidazole). To obtain better datasets, the analyses were performed at 133 K. Attempts to analyse the X-ray structure of [1(HeptIm)₂] at 273 K were not successful. The molecular structures of the two compounds are displayed in Figure 1. [1(HeptIm)₂] and [1(DecIm)₂] crystallise in the triclinic space group *P* $\bar{1}$ with two molecules in the unit cell. Neither compound contains additional solvent molecules in the crystal packing. Selected bond lengths and angles of [1(HeptIm)₂] and [1(DecIm)₂] are listed in Table 1. The length of the bonds to the equatorially coordinated N and O atoms are all ca. 1.9 Å, and the bond lengths to the axially coordinated nitrogen atoms of the imidazole rings are slightly longer (ca. 2.0 Å). The data were collected at 133 K, and the O–Fe–O angles of 89.4° { [1(HeptIm)₂] } and 88.2° { [1(DecIm)₂] } at this temperature in combination with the bond lengths clearly indicate that both complexes reside in the LS state, as similar bond

lengths and angles are observed for other LS complexes of this ligand type.^[16]

The imidazole rings of [1(HeptIm)₂] are almost perpendicular to each other with an angle of 86.4°. The C₇ alkyl chains of both axial ligands point in different directions and span an angle of ca. 90°. Thus, the molecule does not have the expected rodlike structure and is best described as a bent rod. Two contacts shorter than the sum of the van der Waals radii by 0.2 Å are observed between one molecule and a neighbouring molecule, which is oriented upside down. One of these two nonclassical hydrogen bonds occurs between H29 of one imidazole ligand and the oxygen atom O2 of the equatorial ligand directly coordinated to the central iron ion (C29–H29...O2, 2.492 Å). The other nonclassical hydrogen bond connects oxygen atom O3 in the outer periphery of the ligand with the first H atom, H22, of the alkyl chain of the molecule shifted aside. In Table 2, the geometric parameters of the nonclassical hydrogen bonds of the molecules are listed. The angle between the imidazole rings of [1(DecIm)₂] of 76.5° is smaller and more in the region of the angle observed for the MeIm complexes.^[9,10] In contrast to the chains in [1(HeptIm)₂], the C₁₀ alkyl chains point in the same direction (towards O1 of the equatorial ligand) and are slightly bent in opposite directions.

Again, a rodlike structure is not observed, but, owing to the bent alkyl chains, the structure is closer to an amphiphile. One intermolecular contact shorter than the sum of the van der Waals radii by 0.2 Å connects two opposite molecules, which are again oriented upside down. Similarly to the short contact in [1(HeptIm)₂], this contact connects

Table 1. Selected bond lengths [Å] and angles [°] within the inner coordination sphere and spin state of the complexes at 133 K discussed in this work.

	Fe–N _{eq}	Fe–O _{eq}	Fe–N _{ax}	N _{ax} –Fe–N _{ax}	O–Fe–O	Spin state
[1(HeptIm) ₂]	1.870(5), 1.893(5)	1.947(4), 1.935(4)	2.010(5), 1.998(5)	176.06(21)	89.41(15)	LS
[1(DecIm) ₂]	1.983(2), 1.892(2)	1.934(1), 1.932(1)	2.007(2), 1.998(2)	178.88(7)	88.25(6)	LS

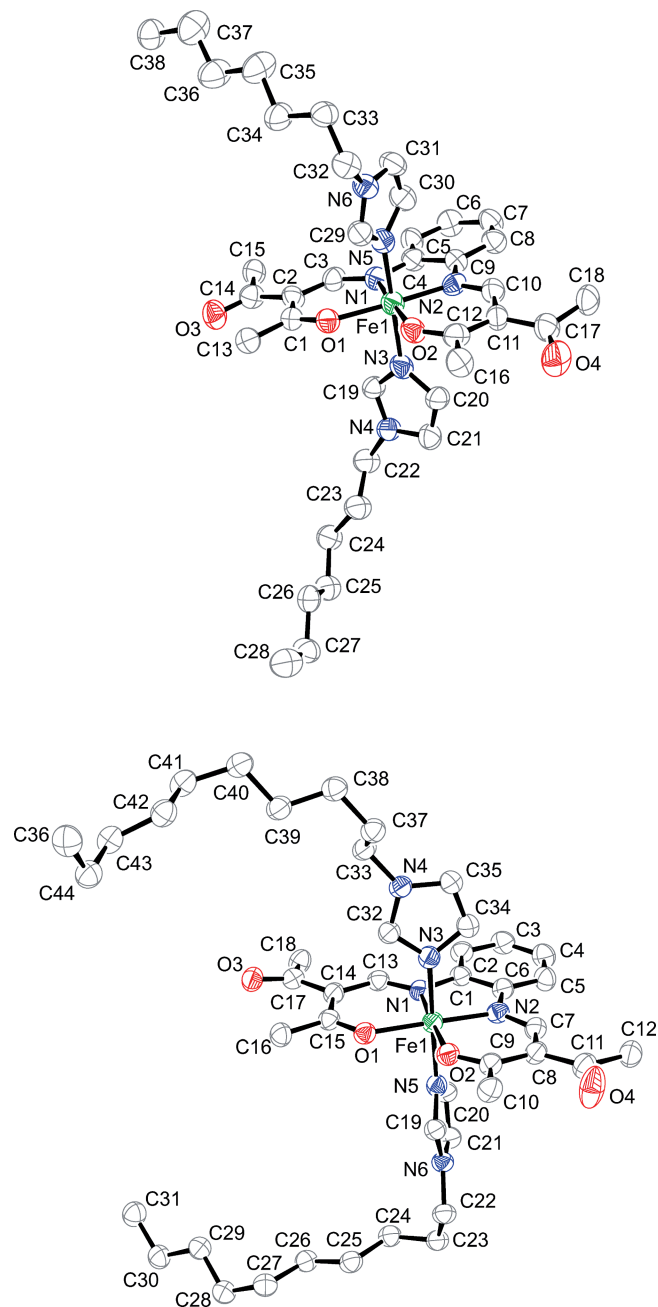


Figure 1. ORTEP drawings of [I(HeptIm)₂] (top) and [I(DecIm)₂] (bottom). The ellipsoids are drawn at the 50% probability level. Hydrogen atoms are omitted for clarity.

Table 2. Distances [Å] and angles [°] of the nonclassical hydrogen bonds in the crystal structures at 133 K.

	D–H...A	D–H	H...A	D...A	D–H...A
[I(HeptIm) ₂]	C22–H22B...O3 ^[a]	0.99	2.54	3.237(8)	127
	C29–H29...O2 ^[b]	0.95	2.49	3.267(8)	139
[I(DecIm) ₂]	C33–H33A...O3 ^[c]	0.99	2.51	3.430(3)	154

[a] $-x, 2 - y, 1 - z$. [b] $1 - x, 2 - y, 1 - z$. [c] $1 - x, 1 - y, -z$.

the H atom of the first carbon atom of one alkyl chain with the oxygen atom O3 in the outer periphery of the equatorial

ligand. As the molecules are orientated towards each other, this nonclassical hydrogen bond is formed.

The packing patterns of [I(HeptIm)₂] and [I(DecIm)₂] are displayed in Figure 2. In the crystal packing of [I(HeptIm)₂], the alkyl chain at the top of one molecule is arranged almost parallel to the same alkyl chain of the neighbouring upside-down molecule. On the other hand, the slightly bent alkyl chain on the bottom of one molecule is arranged next to the slightly bent alkyl chain on the top of the neighbouring upside-down molecule. Despite this structural motif, there are no indications of van der Waals interactions between the alkyl chains.

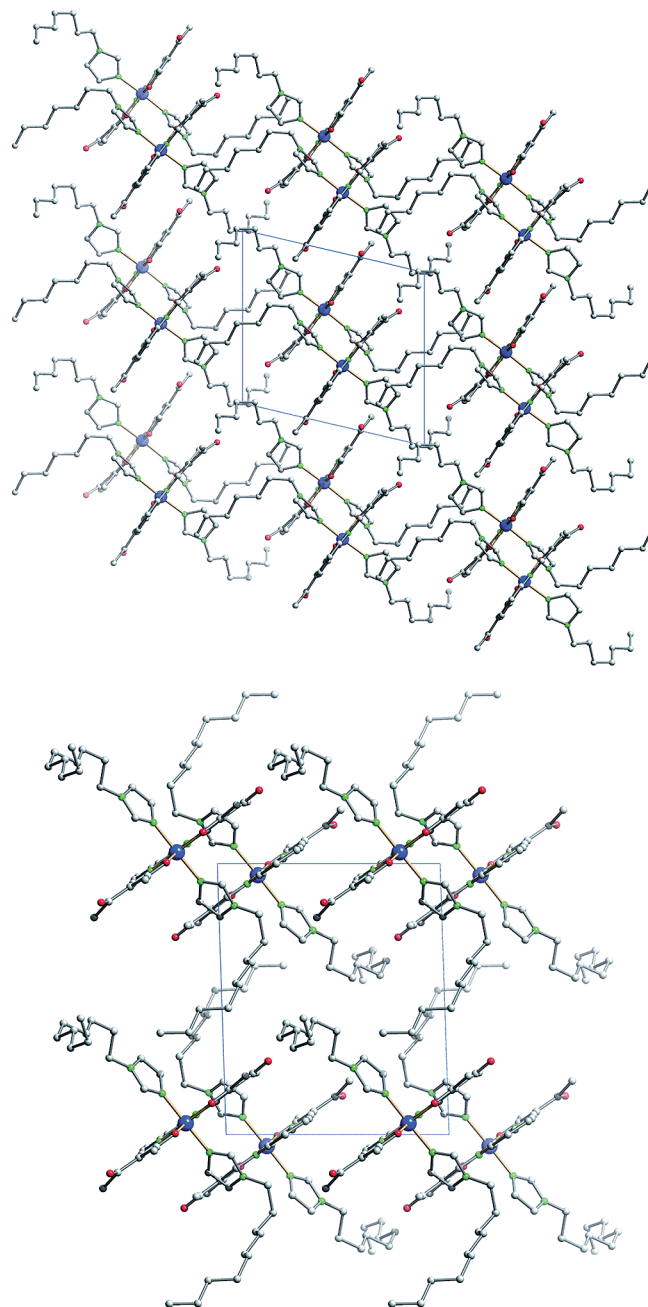


Figure 2. Crystal packing of (top) [I(HeptIm)₂] along [010] and (bottom) [I(DecIm)₂] along [010].

In contrast to [1(HeptIm)₂], some van der Waals interactions are observed in [1(DecIm)₂] between the alkyl chains of one molecule (C23–C31) and the second alkyl chain of a neighbouring complex. Additionally, for the last part of this alkyl chain, some interactions with another, third neighbouring complex molecule (C37–C31) are observed. In Figure 2 (bottom), the crystal packing of [1(DecIm)₂] is displayed, and the closely packed alkyl chains can be seen.

Magnetic Measurements

Solid samples of high enough purity and in sufficient quantities for superconducting quantum interference device (SQUID) magnetometry measurements were obtained for the compounds with the C₅ and C₁₀ chains, [1(PentIm)₂] and [1(DecIm)₂]. The results are plotted in Figure 3. At 300 K, the product of the molar susceptibility and temperature ($\chi_M T$) of [1(PentIm)₂] of 3.19 cm³ K mol⁻¹ is characteristic of a HS state. As the sample is cooled to 185 K, the $\chi_M T$ product slowly decreases and a plateau is observed in the temperature range between 170 and 120 K ($\chi_M T = 2.82$ cm³ K mol⁻¹). At 100 K, the $\chi_M T$ product again decreases to a value of 2.00 cm³ K mol⁻¹ and remains at this value to 20 K, at which point it again decreases rapidly owing to zero-field splitting. The incomplete character of this spin-transition curve could be due to the presence of different polymorphs in the sample, for example, with different PentIm content (see Experimental Section). From other SCO complexes of this ligand system, it is known that the magnetic properties can change drastically as the composi-

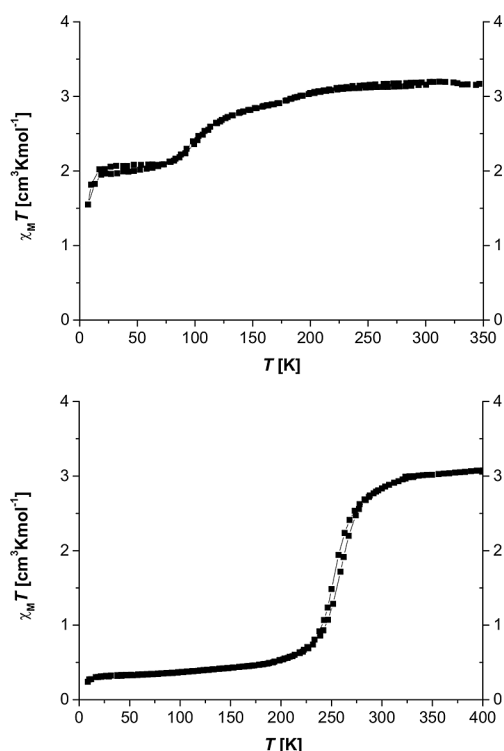


Figure 3. SQUID measurements of [1(PentIm)₂] (top) and [1(DecIm)₂] (bottom).

tion of the material changes.^[17] Another point is that the spin transition occurs at comparably low temperatures; thus, quenching effects are very likely at temperatures below 100 K. A similar behaviour was observed previously for other complexes of this ligand system.^[18]

The room-temperature $\chi_M T$ product of [1(DecIm)₂] ($\chi_M T = 2.83$ cm³ K mol⁻¹) shows that the compound is not fully in the HS state at this temperature. As the temperature decreases, $\chi_M T$ decreases first gradually, then rapidly, and then gradually again until a value of 0.54 cm³ K mol⁻¹ at 200 K is obtained. This corresponds to a LS state of the system with $T_{1/2}^{\downarrow} = 254$ K. Below this temperature, the $\chi_M T$ product decreases very gradually to 0.32 cm³ K mol⁻¹ at 25 K. As the temperature increases, the curve progression of the $\chi_M T$ product corresponds almost exactly to the values in the cooling mode. In the more abrupt region, the increase of the $\chi_M T$ product occurs at a slightly higher temperature ($T_{1/2}^{\uparrow} = 259$ K), which results in a small hysteresis of 5 K. Upon further heating to 400 K, the full HS state ($\chi_M T = 3.06$ cm³ K mol⁻¹) is reached. The SCO curve progression is more abrupt for [1(DecIm)₂], for which a network of van der Waals interactions between the alkyl chains is observed. The complete spin transition is in good agreement with the results from the X-ray structure analysis (low spin at 133 K).

Additionally, we determined the temperature-dependent magnetic susceptibilities of the iron complex **1** bearing axially coordinated alkylimidazole ligands with different alkyl chain lengths of 1, 5, 7 and 10 carbon atoms in methanol/alkylimidazole solutions. This allowed us to study the influence of the alkyl chain length and packing effects on the spin-transition properties. The concentrations of the complexes in the solutions were ca. 38–55 mg/mL (methylimidazole to decylimidazole). The presence of the octahedral complexes in solution was confirmed by colour changes upon cooling owing to the spin transition (see Supporting Information, Figure S1). The results are plotted in Figure 4. The spin-transition behaviour for all complexes is identical. The gradual progression is typical of SCO in solution, in which all of the cooperative effects that are responsible for a rapid switch of the spin state are switched off. This proves

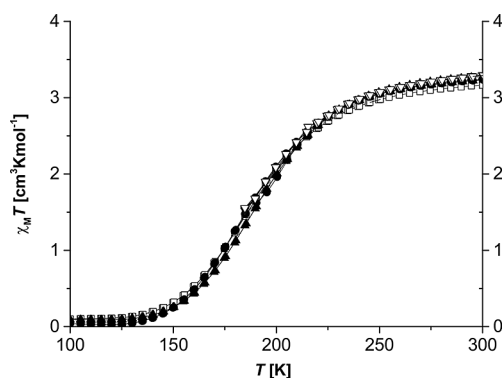


Figure 4. SQUID measurements of solutions of [1(MeIm)₂] (open squares), [1(PentIm)₂] (circles), [1(HeptIm)₂] (triangles) and [1(DecIm)₂] (open triangles).

that packing effects (e.g., different orientations of the axial ligand, short contacts) are responsible for the differences in the SCO behaviour of the solids.

Conclusions

In this article, we present a new class of iron(II) spin-crossover coordination compounds with Schiff base like equatorial ligands and alkylimidazoles with different chain lengths as axial ligands. The alkyl chain lengths were varied from 1 to 5, 7 and 10 carbon atoms. The crystal structures of [1(HeptIm)₂] and [1(DecIm)₂] were obtained, and the molecules show a very similar crystal packing. Pairs of molecules oriented upside down relative to each other are strongly connected by nonclassical hydrogen bonds. In contrast to those in [1(HeptIm)₂], the alkyl chains in [1(DecIm)₂] interact with each other and are, therefore, arranged parallel to each other. [1(PentIm)₂] shows a rather gradual and stepwise incomplete spin transition with plateaus, whereas [1(DecIm)₂] exhibits a relatively abrupt spin crossover with 5 K wide hysteresis, centred at 257 K. Thus, with increasing alkyl chain length, increased cooperative interactions between the spin-crossover centres are observed owing to the improvement in conditions for van der Waals interactions. This observation is in excellent agreement with the results obtained for related complexes with amphiphilic Schiff base like ligands.^[6c,7] Magnetic measurements of the complexes in solution with alkylimidazoles bearing different alkyl chain lengths prove the absence of cooperative effects in solution, and almost identical behaviour is observed for all complexes.

Experimental Section

General: The syntheses of the iron complexes were performed under an argon atmosphere by Schlenk techniques. The solvents were purified and distilled under an atmosphere of argon.^[19] The alkyl bromides were commercial products (Sigma–Aldrich) and used as received. The syntheses of the precursors ethoxymethyleneacetylacetone^[20] and iron(II) acetate^[21] have been described previously. For the synthesis of the alkylimidazoles, slightly modified literature procedures were used.^[11–13]

N-Pentylimidazole: Imidazole (34.04 g, 0.5 mol) was dissolved in methanol (45 mL), and an aqueous KOH solution (50%, 100 mL) was added. The mixture was heated to 85 °C, and 1-bromopentane (75.52 g, 0.5 mol) was added dropwise under vigorous stirring over 4 h. After cooling to room temp., the two-phase mixture was separated from the solid, and the solvent was evaporated. Chloroform (300 mL) was added slowly, and the solution was filtered at room temp. The product was dried over Na₂SO₄ overnight and distilled at 100 °C and 5 × 10⁻⁴ bar, yield 35.6 g (52%). MS (DEI+): *m/z* (%) = 138 (72) [M]⁺. ¹H NMR (CDCl₃, 399.8 MHz): δ = 0.89 (t, CH₃), 1.30 [m, (CH₂)₂], 1.77 (q, NCH₂CH₂), 3.92 (t, NCH₂), 6.90 [s, (Im)NCHCHN], 7.04 [s, (Im)NCHCHN], 7.45 [s, (Im)NCHN] ppm.

N-Heptylimidazole: Imidazole (20.42 g, 0.3 mol) was dissolved in methanol (32 mL), and an aqueous KOH solution (50%, 65 mL) was added. The mixture was heated to 100 °C, and 1-bromoheptane (43.73 g, 0.3 mol) was added dropwise under vigorous stirring

over 3.5 h. After cooling to room temp., the two-phase mixture was separated from the solid, and the solvent was evaporated. Chloroform (100 mL) was added slowly, and the solution was filtered at room temp. The product was dried over Na₂SO₄ overnight and distilled at 155 °C and 3 × 10⁻⁴ bar, yield 28.3 g (57%). MS (DEI+): *m/z* (%) = 166 (36) [M]⁺. ¹H NMR (CDCl₃, 399.8 MHz): δ = 0.81 (t, CH₃), 1.22 [m, (CH₂)₄], 1.70 (q, NCH₂CH₂), 3.85 (t, NCH₂), 6.84 [s, (Im)NCHCHN], 6.98 [s, (Im)NCHCHN], 7.39 [s, (Im)NCHN] ppm.

N-Decylimidazole: Imidazole (34.04 g, 0.5 mol) was dissolved in methanol (45 mL), and an aqueous KOH solution (50%, 100 mL) was added. The mixture was heated to 90 °C, and 1-bromodecane (110.59 g, 0.5 mol) was added dropwise under vigorous stirring over 4 h. After cooling to room temp., the two-phase mixture was separated from the solid, and the solvent was evaporated. Chloroform (300 mL) was added slowly, and the solution was filtered at room temp. The product was dried over Na₂SO₄ overnight and distilled twice at 145 °C and 3.5 × 10⁻⁴ bar, yield 82.97 g (80%). ¹H NMR (CDCl₃, 399.8 MHz): δ = 0.89 (t, CH₃), 1.20 [m, (CH₂)₂], 1.71 (q, NCH₂CH₂), 3.87 (t, NCH₂), 6.85 [s, (Im)NCHCHN], 6.99 [s, (Im)NCHCHN], 7.41 [s, (Im)NCHN] ppm.

[1(DecIm)₂]: [1(MeOH)₂] (0.62 g, 1.40 mmol) and DecIm (2.5 mL) were heated to reflux in methanol (4 mL) for 70 min. The reddish-black solution was stored at -28 °C. The solution was then decanted at -27 °C from the black blocklike crystals. C₄₄H₆₆FeN₆O₄·0.75DecIm·1.5MeOH (1003.20): calcd. C 66.15, H 9.04, N 10.47; found C 66.32, H 8.53, N 10.64. IR: ν̄ = 2923 (vs, CH₂), 2854 (s, CH₂), 1635 (m, CO), 1560 (vs, CO), 1393 (s), 1274 (s), 1228 (s), 1076 (s) cm⁻¹.

[1(PentIm)₂]: [1(MeOH)₂] (0.55 g, 1.23 mmol) and PentIm (2.0 mL) were heated to reflux in methanol (4 mL) for 3 h 15 min. The reddish-black solution was stored at -28 °C. The solution was then decanted at -27 °C from the black precipitate. C₃₄H₄₆FeN₆O₄·3PentIm·MeOH (1105.28): calcd. C 64.11, H 8.39, N 15.21; found C 63.86, H 8.05, N 15.52. IR: ν̄ = 2931 (s, CH₂), 2861 (m, CH₂), 1627 (s, CO), 1556 (vs, CO), 1382 (vs), 1271 (vs), 1229 (s), 1079 (s) cm⁻¹.

[1(HeptIm)₂]: [1(MeOH)₂] (1.58 g, 4.13 mmol) and HeptIm (10.0 mL) were heated to 90 °C for 6 h. After several cycles of storing at 5 and 25 °C, a black precipitate could be isolated. In the remaining solution, black needles crystallised at -30 °C. C₃₈H₅₄FeN₆O₄·6HeptIm (1712.13): calcd. C 68.74, H 9.54, N 14.72; found C 68.59, H 9.76, N 16.75. IR: ν̄ = 2925 (s, CH₂), 2857 (m, CH₂), 1652 (s, CO), 1563 (s, CO), 1391 (vs), 1271 (m), 1225 (vs), 1075 (vs) cm⁻¹.

Preparation of the Solutions: [1(MeOH)₂] (0.202 g, 0.45 mmol) was dissolved in the different alkylimidazoles (methylimidazole, pentylimidazole, heptylimidazole and decylimidazole; 2.5 mL), and the red solutions were heated to 150 °C for 1 h. The solutions were cooled to room temperature, and methanol (4 mL) was added. For the SQUID samples, 0.05 mL of each solution was used.

Magnetic Susceptibilities: The data for [1(PentIm)₂] and [1(DecIm)₂] were collected with a Quantum Design MPMS-XL5 SQUID magnetometer under an applied field of 0.05 T over 10–400 K in the sweep mode. All samples were placed in gelatine capsules held within plastic straws. The data were corrected for the diamagnetic magnetisation of the ligands, which were estimated from Pascal's constants, and the sample holder. The outcomes from elemental analysis were used to determine the exact molecular weight per iron centre. For the measurements in solution, the samples were sealed in the plastic straws and measured in the settle

mode with an applied field of 0.2 T. The raw data were corrected for the diamagnetism of the solution and the diamagnetism of the organic ligand by using tabulated Pascal's constants.

X-ray Diffraction: The intensity data of [I(HeptIm)₂] and [I(DecIm)₂] were collected with a Stoe IPDS II diffractometer at 133 K with graphite-monochromated Mo-K_α radiation. The data were corrected for Lorentz and polarisation effects. The structures were solved by direct methods {Sir2011^[22] for [I(HeptIm)₂], Sir97^[23] for [I(DecIm)₂]} and refined by full-matrix least-square techniques against F_o² (SHELXL-97).^[24] The hydrogen atoms were included at calculated positions with fixed displacement parameters. All non-hydrogen atoms were refined anisotropically. ORTEP-III^[25] was used to prepare the structure representation, and Schakal-99^[26] and Mercury^[27] were used to prepare the representations of the molecule packing.

CCDC-1016502 {for [I(HeptIm)₂]} and -1016503 {for [I(DecIm)₂]} contain the supplementary crystallographic data for this paper. These data can be obtained free of charge from The Cambridge Crystallographic Data Centre via www.ccdc.cam.ac.uk/data_request/cif.

Elemental Analysis: Elemental analysis was performed with a VarioEL III CHN instrument and tin boats purchased from Elementar, and acetanilide (Merck) were used as the standard.

Acknowledgments

Support from the University of Bayreuth, the Deutsche Forschungsgemeinschaft (DFG) (WE 3546_4-1) and the Fonds der Chemischen Industrie is gratefully acknowledged.

- [1] a) M. A. Halcrow (Ed.), *Spin-Crossover Materials*, John Wiley & Sons, Chichester, UK, **2013**; b) P. Gütllich, H. Goodwin (Eds.), *Spin Crossover in Transition Metal Compounds I–III*, Springer, Berlin, **2004**; c) J. Linares, E. Codjovi, Y. Garcia, *Sensors* **2012**, *12*, 4479–4492; d) A. Bousseksou, G. Molnar, L. Salmon, W. Nicolazzi, *Chem. Soc. Rev.* **2011**, *40*, 3313–3335; e) M. C. Muñoz, J. A. Real, *Coord. Chem. Rev.* **2011**, *255*, 2068–2093; f) J. Olguin, S. Brooker, *Coord. Chem. Rev.* **2011**, *255*, 203–240; g) A. B. Koudriavtsev, W. Linert, *J. Struct. Chem.* **2010**, *51*, 335–365; h) S. Brooker, J. A. Kitchen, *Dalton Trans.* **2009**, 7331–7340; i) J. Klingele, D. Kaase, M. Schmucker, Y. Lan, G. Chastanet, J.-F. Létard, *Inorg. Chem.* **2013**, *52*, 6000–6010; j) S. Heider, H. Petzold, G. Chastanet, S. Schlamp, T. Rüffer, B. Weber, J.-F. Létard, *Dalton Trans.* **2013**, *42*, 8575–8584; k) S. K. Hain, F. W. Heinemann, K. Gieb, P. Müller, G. Hörner, A. Grohmann, *Eur. J. Inorg. Chem.* **2010**, 221–232; l) M. Milek, F. W. Heinemann, M. M. Khusniyarov, *Inorg. Chem.* **2013**, *52*, 11585–11592; m) K. S. Murray, *Aust. J. Chem.* **2009**, *62*, 1081–1101; n) A. Gaspar, M. Seredyuk, P. Gütllich, *J. Mol. Struct.* **2009**, *924–926*, 9–19; o) J.-F. Létard, *J. Mater. Chem.* **2006**, *16*, 2550–2559; p) O. Sato, J. Tao, Y.-Z. Zhang, *Angew. Chem. Int. Ed.* **2007**, *46*, 2152–2187; *Angew. Chem.* **2007**, *119*, 2200; q) B. Weber, in: *Spin-Crossover Materials* (Ed.: M. A. Halcrow), John Wiley & Sons, Chichester, UK, **2013**, p. 55–76.
- [2] a) Y. Bodenthin, U. Pietsch, H. Möhwald, D. G. Kurth, *J. Am. Chem. Soc.* **2005**, *127*, 3110–3114; b) T. Fujigaya, D.-L. Jiang, T. Aida, *Chem. Asian J.* **2007**, *2*, 106–113; c) M. Seredyuk, A. B. Gaspar, V. Ksenofontov, Y. Galyametdinov, J. Kusz, P. Gütllich, *Adv. Funct. Mater.* **2008**, *18*, 2089–2101; d) J. A. Kitchen, N. G. White, C. Gandolfi, M. Albrecht, G. N. L. Jameson, J. L. Tallon, S. Brooker, *Chem. Commun.* **2010**, *46*, 6464.
- [3] a) H. Matsukizono, K. Kuroiwa, N. Kimizuka, *J. Am. Chem. Soc.* **2008**, *130*, 5622–5623; b) A. B. Gaspar, M. Seredyuk, P. Gütllich, *Coord. Chem. Rev.* **2009**, *253*, 2399–2413; c) P. N. Martinho, C. J. Harding, H. Müller-Bunz, M. Albrecht, G. G. Morgan, *Eur. J. Inorg. Chem.* **2010**, 675–679; d) Y. Garcia, B.-L. Su, Y. Komatsu, K. Kato, Y. Yamamoto, H. Kamihata, Y. H. Lee, A. Fuyuhiko, S. Kawata, S. Hayami, *Eur. J. Inorg. Chem.* **2012**, 2769–2775.
- [4] Y. H. Lee, A. Ohta, Y. Yamamoto, Y. Komatsu, K. Kato, T. Shimizu, H. Shinoda, S. Hayami, *Polyhedron* **2011**, *30*, 3001–3005.
- [5] a) P. N. Martinho, Y. Ortin, B. Gildea, C. Gandolfi, G. McKerr, B. O'Hagan, M. Albrecht, G. G. Morgan, *Dalton Trans.* **2012**, *41*, 7461–7463; b) C. Gandolfi, C. Moitzi, P. Schurtenberger, G. G. Morgan, M. Albrecht, *J. Am. Chem. Soc.* **2008**, *130*, 14434–14435.
- [6] a) S. Schlamp, K. Dankhoff, B. Weber, *New J. Chem.* **2014**, *38*, 1965–1972; b) S. Schlamp, P. Thoma, B. Weber, *Chem. Eur. J.* **2014**, *20*, 6462–6473; c) S. Schlamp, P. Thoma, B. Weber, *Eur. J. Inorg. Chem.* **2012**, 2759–2768.
- [7] S. Schlamp, B. Weber, A. D. Naik, Y. Garcia, *Chem. Commun.* **2011**, *47*, 7152–7154.
- [8] a) S. Hayami, Y. Komatsu, T. Shimizu, H. Kamihata, Y. H. Lee, *Coord. Chem. Rev.* **2011**, *255*, 1981–1990; b) S. Hayami, N. Motokawa, A. Shuto, R. Moriyama, N. Masuhara, K. Inoue, Y. Maeda, *Polyhedron* **2007**, *26*, 2375–2380; c) S. Hayami, R. Moriyama, A. Shuto, Y. Maeda, K. Ohta, K. Inoue, *Inorg. Chem.* **2007**, *46*, 7692–7694; d) S. Hayami, Y. Kojima, D. Urakami, K. Ohta, K. Inoue, *Polyhedron* **2009**, *28*, 2053–2057.
- [9] B. Weber, E. S. Kaps, J. Obel, K. Achterhold, F. G. Parak, *Inorg. Chem.* **2008**, *47*, 10779–10787.
- [10] B. Weber, E. Kaps, J. Obel, W. Bauer, *Z. Anorg. Allg. Chem.* **2008**, *634*, 1421–1426.
- [11] M. Häring, *Helv. Chim. Acta* **1959**, *42*, 1845–1846.
- [12] E. Bäuerlein, H. Träsch, *Liebigs Ann. Chem.* **1979**, 1818–1827.
- [13] C. F. Wilkinson, K. Hetnarski, G. P. Cantwell, F. J. Di Carlo, *Biochem. Pharmacol.* **1974**, *23*, 2377–2386.
- [14] L. Wolf, E.-G. Jäger, *Z. Anorg. Allg. Chem.* **1966**, *346*, 76–91.
- [15] B. Weber, E.-G. Jäger, *Z. Anorg. Allg. Chem.* **2009**, *635*, 130–133.
- [16] a) B. Weber, E.-G. Jäger, *Eur. J. Inorg. Chem.* **2009**, 465–477; b) B. Weber, *Coord. Chem. Rev.* **2009**, *253*, 2432–2449; c) T. M. Pfaffeneder, S. Thallmair, W. Bauer, B. Weber, *New J. Chem.* **2011**, *35*, 691–700.
- [17] B. Weber, E. S. Kaps, C. Desplanches, J. Létard, *Eur. J. Inorg. Chem.* **2008**, 2963–2966.
- [18] W. Bauer, W. Scherer, S. Altmannshofer, B. Weber, *Eur. J. Inorg. Chem.* **2011**, 2803–2818.
- [19] H. G. O. Becker, *Organikum: Organisch-chemisches Grundpraktikum*, Johann Ambrosius Barth, Berlin, **1993**.
- [20] L. Claisen, *Justus Liebigs Ann. Chem.* **1897**, *297*, 1–98.
- [21] B. Weber, R. Betz, W. Bauer, S. Schlamp, *Z. Anorg. Allg. Chem.* **2011**, *637*, 102–107.
- [22] M. C. Burla, R. Caliendo, M. Camalli, B. Carrozzini, G. L. Cascarano, C. Giacovazzo, M. Mallamo, A. Mazzone, G. Polidori, R. Spagna, *J. Appl. Crystallogr.* **2012**, *45*, 357–361.
- [23] A. Altomare, M. C. Burla, M. Camalli, G. L. Cascarano, C. Giacovazzo, A. Guagliardi, A. G. G. Moliterni, G. Polidori, R. Spagna, *J. Appl. Crystallogr.* **1999**, *32*, 115–119.
- [24] G. Sheldrick, *Acta Crystallogr., Sect. A* **2008**, *64*, 112–122.
- [25] a) L. Farrugia, *J. Appl. Crystallogr.* **1997**, *30*, 565; b) C. K. Johnson, M. N. Burnett, *ORTEP-III*, Oak Ridge National Laboratory, Oak Ridge, **1996**.
- [26] E. Keller, *Schakal-99*, University of Freiburg, Germany, **1999**.
- [27] C. F. Macrae, P. R. Edgington, P. McCabe, E. Pidcock, G. P. Shields, R. Taylor, M. Towler, J. van de Streek, *J. Appl. Crystallogr.* **2006**, *39*, 453–457.

Received: October 27, 2014

Published Online: ■

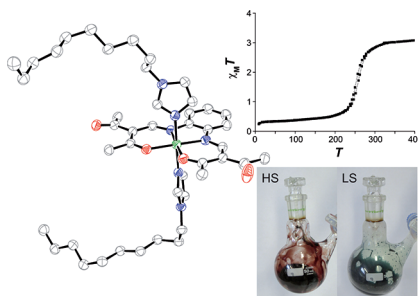
Spin-Crossover Complexes

S. Schlamp, C. Lochenie, T. Bauer,
R. Kempe, B. Weber* 1–7



Iron(II) Spin-Crossover Complexes with Schiff Base Like Ligands and *N*-Alkylimidazoles

Keywords: Iron / Spin crossover / Schiff base ligands / N ligands



Iron(II) spin-crossover complexes with Schiff base like equatorial ligands and alkylimidazole axial ligands are synthesised. The alkyl chain length is varied from 5 to 7 and 10 carbon atoms. The crystal structures of the C_7 and C_{10} compounds are described. There is an increased cooperativity in spin-crossover behaviour for the compound with the longer C_{10} alkyl chain than for the C_5 compound.